

Highlights

Reducing RES Droughts through the integration of wind and PV

Boris Morin, Aina Maimó Far, Damian Flynn, Conor Sweeney

- RES droughts are analysed using 45 years of hourly wind and PV generation data
- RES droughts from C3S-Energy and ERA5-Atlite datasets are compared
- Adding PV to a wind-dominated system reduces RES drought frequency and duration
- Validated RES datasets are crucial to accurately identify RES drought extremes

Reducing RES Droughts through the integration of wind and PV

Boris Morin^{a,*}, Aina Maimó Far^a, Damian Flynn^b, Conor Sweeney^a

*^aSchool of Mathematics and Statistics, University College Dublin, Belfield, Dublin
4, Dublin, D04 V1W8, Ireland*

*^bSchool of Electrical and Electronic Engineering, University College Dublin, Belfield,
Dublin 4, Dublin, D04 V1W8, Ireland*

*Corresponding author

Email addresses: `boris.morin@ucdconnect.ie` (Boris Morin),
`aina.maimofar@ucd.ie` (Aina Maimó Far), `damian.flynn@ucd.ie` (Damian Flynn),
`conor.sweeney@ucd.ie` (Conor Sweeney)

Abstract

Increasing the share of electricity produced from renewable energy sources (RES), combined with RES dependence on weather, poses a critical challenge for energy systems. This study investigates the importance of the balance between wind and photovoltaic (PV) capacity on periods of low renewable generation, known as RES droughts. Three different RES models are used to estimate the capacity factors for different scenarios of installed capacities for wind and PV power. The skill of the RES models is quantified by comparing capacity factor time series to observed hourly data and by assessing their representation of observed RES droughts. The RES models are used to generate a 45-year hourly time series of RES capacity factor, enabling analysis of the frequency, duration and return periods of RES droughts at a climatological scale. Results show the importance of using an accurate, validated RES model for RES drought risk assessment. The addition of PV capacity to a wind-dominated system results in a significant reduction in the frequency and duration of RES droughts, while also reducing extremes and seasonal drought patterns. These findings underscore the importance of diversification in RES capacity to enhance energy security and resilience.

Keywords: RES Drought, Wind Power, Solar PV Power, Renewable Energy Sources, Return Periods

1. Introduction

The EU aims to generate at least 69% of its electricity from renewable energy sources (RES) by 2030, up from 41% in 2022 [1]. While this transition is essential for reducing greenhouse gas emissions, it also highlights the challenge of managing the variability of weather-dependent energy sources such as wind and photovoltaic (PV) power. This challenge is amplified by the increasing electrification of energy sectors, which places greater demand on the power system and makes it more sensitive to meteorological conditions, both in historical [2] and future climates [3]. Periods of low renewable generation, known as *Dunkelflaute* or RES droughts, pose significant risks to system adequacy and energy security, emphasising the need for a resilient energy system to meet both growing electricity demand and decarbonisation targets.

14 This study focuses on Ireland, a region with a strong reliance on wind
15 power, which has ambitious targets for PV power expansion. This case study
16 provides valuable insights into the potential benefits of diversifying the re-
17 newable energy mix on RES droughts. The performance of different RES
18 datasets are compared, and a 45-year time series of RES generation is pro-
19 duced. The results highlight the role of increased PV capacity in reducing
20 RES drought risks, offering insights for policymakers and energy planners.

21 For this study, a RES drought event is defined as occurring when the
22 average capacity factor (CF) remains below a fixed threshold for a given
23 duration, following the methodology used in previous research. Kaspar et
24 al. [4] analysed the shortfall risks of low wind and PV in Europe, with a
25 focus on Germany. Mockert et al. [5] expanded on this by examining the
26 link between weather regimes and RES droughts in Germany. Similar anal-
27 yses were conducted using machine learning for Japan [6] and Hungary [7].
28 Alternative methods exist for defining RES droughts. One approach uses rel-
29 ative CF thresholds that adjust throughout the year to account for seasonal
30 variations in renewable electricity generation. Raynaud et al. [8] defined a
31 drought as a sequence of days with energy production below a threshold,
32 applying this method over a number of European regions. This methodol-
33 ogy was later used to study wind and PV droughts in India using machine
34 learning methods [9]. Kapica et al. [10] built upon this approach to compare
35 the likelihood of RES droughts increasing in Europe under different climate
36 models. Rinaldi et al. [11] instead defined RES droughts as periods when
37 wind or PV CF falls below a percentage of the daily mean for that time of
38 year and assessed RES drought risks in the U.S. Western Interconnection.
39 Also focusing on the U.S., Brown et al. [12] used a weekly timescale rather
40 than hourly or daily data and examined RES droughts from a meteorological
41 perspective. Another method defines energy drought indices based on met-
42 rics commonly used in hydro-meteorology to characterise RES droughts [13].
43 This approach identifies periods of unusually low generation relative to his-
44 torical production levels, using the lowest production percentiles. It has been
45 applied in other studies, including analyses of RES droughts in the U.S. [14]
46 and China [15]. In addition to examining periods of low renewable electricity
47 generation, Raynaud et al. [8] analysed the imbalance between electricity de-
48 mand and renewable generation, known as residual load. These events were
49 studied alongside low-generation periods to assess their correlation. Similar
50 analyses have been conducted in Europe [13] and the U.S. [14], revealing
51 differing results across regions.

In this paper, the focus is exclusively on renewable electricity generation, and a fixed threshold approach to define RES droughts is used, which facilitates consistent inter-comparison between scenarios with different installed wind and PV capacities.

RES droughts are identified using onshore wind and PV CF time series. In this study, three different datasets are used, all of which are driven by ERA5 data [16]. Two of the datasets are part of C3S Energy (C3S-E), an energy-based operational dataset produced by the EU Copernicus Climate Change Service [17]. One of the C3S-E datasets provides CF time series aggregated at the national scale, while the other provides the CF time series at each grid point, at the ERA5 resolution of 0.25° . The third dataset was generated using the Atlite model [19], which converts the ERA5 atmospheric data to a generation time series using specified wind turbine and PV panel models. Atlite is an open-source tool developed by PyPSA [19] and has been used for estimating wind and PV generation in order to study RES droughts [5].

The datasets used in this study are detailed in section 2, which describes their characteristics and relevance for evaluating RES droughts. Section 3 outlines the RES datasets used to simulate wind and PV generation and provides the methodology for defining and identifying RES drought events, including the thresholds and metrics applied. In section 4, the datasets are first verified against observed energy data to assess their accuracy, followed by an analysis of RES drought occurrences for two scenarios with different ratios of installed wind to PV capacities. Finally, section 5 offers a discussion of the results in the context of energy reliability and future planning, followed by the main conclusions and recommendations for further research.

2. Data

This study uses publicly available datasets to construct and validate the datasets for estimating the CF of wind and PV energy. The primary data sources include: EirGrid and SONI, the transmission system operators (TSO) for the Republic of Ireland and Northern Ireland, respectively; the ERA5 reanalysis dataset; and the C3S-E datasets.

2.1. Wind and PV Capacity and Availability

EirGrid, the TSO for the Republic of Ireland, and SONI, the Northern Ireland TSO, provide detailed datasets on all wind and PV farms across the

island of Ireland (Republic of Ireland and Northern Ireland) from 1990 to the present [23]. These datasets include information such as each farm’s installed capacity, name, and connection date. To enhance the accuracy of this data, the longitude and latitude for each farm were manually determined through online searches. For simplicity, this data will be referred to as originating from EirGrid, as all-island data was directly obtained from EirGrid, and the combined regions of the Republic of Ireland and Northern Ireland will be referred to as Ireland throughout the remainder of this document.

The spreadsheet available from the EirGrid website contains two key variables: generation and availability. Generation is the energy that a RES farm actually contributed to the grid, which may include limitations introduced by the TSO to maintain grid stability, such as constraints and curtailment. Availability represents the energy that would have been generated from a RES farm if no grid constraints had been applied, making it representative of the weather-related response. Generation and availability values are available from 2014 onward for wind power and from 2018 onward for PV power, although PV availability data only became present in the Republic of Ireland in 2023. This study focuses on availability for all analyses.

2.2. Atmospheric Variables

Atlite and C3S-E datasets are driven by the ERA5 reanalysis [16], produced by the European Centre for Medium-Range Weather Forecasts (ECMWF). This global gridded dataset provides hourly atmospheric variables from 1940 to the present at a horizontal resolution of 0.25°. It is widely used for estimating solar and wind energy [5, 17, 12, 24]. Table 1 lists the ERA5 variables used by Atlite and C3S-Energy.

Table 1: ERA5 variables used to calculate wind and PV generation

ERA5 name	variable
100 metre zonal and meridional wind speed	u_{100}, v_{100}
2 metre temperature	$t2m$
Surface net solar radiation	ssr
Surface solar radiation downwards	$ssrd$
Top of atmosphere incident radiation	$tisr$
Total sky direct solar radiation at surface	$fdir$

112 2.3. C3S Energy

113 The EU Copernicus Climate Change Service developed the C3S-E renew-
114 able energy dataset for Europe [17], using ERA5 atmospheric variables and
115 weather-to-energy models. This dataset provides hourly CF for wind and PV
116 energy from 1979 to the present. The data are available on the same grid as
117 the ERA5 data, which has a horizontal resolution of 0.25° . The time series
118 are also available for download at two aggregated scales: regional (NUTS 2)
119 and national.

120 The wind CF in the C3S-E model is calculated using wind speeds at 100
121 metres (u_{100} , v_{100}) and a standard turbine model, the Vestas V136/3450,
122 with a fixed hub height of 100 meters. This choice reflects trends in wind
123 turbine installations and was guided by expert recommendations. Since real-
124 time data on the exact wind turbine fleet across Europe is difficult to obtain,
125 C3S-E assumes a homogeneous distribution of turbines across the ERA5 grid.
126 While this approach does not capture the precise capacity factors reported
127 by grid operators, it provides a well-correlated time series that effectively
128 represents the impact of climate variability on wind power generation. The
129 turbine power curves used in the model are sourced from publicly available
130 databases, ensuring consistency with industry standards. The PV CF in the
131 C3S-E model is calculated at the grid level and represents the aggregated
132 output of all PV systems within each pixel, rather than a single installa-
133 tion. It is derived from meteorological data, including surface solar radiation
134 downwards ($ssrd$) and air temperature ($t2m$), using a reference PV plant
135 model. This model incorporates empirical calculations for key system com-
136 ponents such as optical losses, module efficiency, and inverters. The final
137 capacity factor accounts for a mix of module orientations typical for each
138 location [25].

139 3. Methods

140 This study uses three datasets to analyse RES droughts across the island
141 of Ireland. Data downloaded from C3S-E were used to obtain two datasets:
142 one based on national-level data (C3S-E N), and another on grid-level data
143 (C3S-E G). The third dataset was computed using the Atlite model (Atlite).

144 3.1. C3S-Energy National

145 For national-level analyses, the aggregated CF time series provided by
146 C3S-E were used at two levels: Republic of Ireland (NUTS0: IE) and North-

ern Ireland (NUTS2: UKN0). These are based on the assumption by C3S-E that RES generation occurs at every ERA5 grid point in Ireland. We computed a weighted average of these, based on the installed capacity of each one, to represent the total CF for Ireland.

3.2. C3S-E Gridded

The gridded dataset from C3S-E was used to create CF datasets which account for the location of RES farms in Ireland. A list of the RES farms in Ireland was compiled, including each farm’s latitude, longitude and installed capacity. Using these coordinates, the nearest grid point on the C3S-E grid was identified for each farm. The CF values from the C3S-E dataset corresponding to these grid points were retrieved. A weighted average of the CF values was calculated, with the installed capacity of each farm serving as the weight, to construct the CF time series for Ireland. This process resulted in a time series of RES generation for each energy source (wind and PV) for Ireland, which takes the location of the RES farms into account.

3.3. Atlite

Atlite transforms weather data into energy data using the gridded ERA5 data and the locations of existing RES farms, as described in C3S-E G. ERA5 data for wind speed at 100 metres (u_{100} , v_{100}) are used to calculate wind generation, while the ERA5 radiation variables (ssr , $ssrd$, $tisr$, and $fdir$) and air temperature ($t2m$) are used to calculate PV generation. A key distinction between C3S-E and Atlite lies in their representation of wind turbines and PV panels. This study identifies the most appropriate wind turbine power curve to use from the 121 power curves made available by Renewables.ninja [26]. The selection of a specific wind turbine and PV panel characteristics is further discussed and explained in section 4.1.

3.4. Energy Scenarios

In addition to analysing wind and PV generation separately, a combined CF was computed for each dataset by averaging wind and PV generation, weighted by their installed capacities at the end of 2023 (5.9 GW for wind power and 0.6 GW for PV power). This configuration is referred to as the 91W-9PV scenario, reflecting the distribution of 91% wind and 9% PV capacity. Given that PV capacity in Ireland is low in 2023, and to explore how a more balanced distribution of wind and PV capacities might impact RES

181 droughts, this study also considered a second scenario, referred to as 57W-
 182 43PV, where the installed PV capacity is assumed to increase to 8.6 GW,
 183 while wind capacity rises to 11.45 GW. These values are based on targets
 184 outlined in the roadmap published by the 2024 Climate Action Plan [27].
 185 This study does not include offshore wind in the analysis. Recent reports
 186 suggest that even by 2030, Ireland is unlikely to have any significant new off-
 187 shore wind farms, with projected offshore capacity expected to remain near
 188 zero using realistic scenarios [28].

189 New time series were generated for both the Atlite and C3S-E G PV
 190 datasets, incorporating a revised distribution of installed capacity across Ire-
 191 land as specified in the roadmap. For wind power, the CF time series remains
 192 unchanged, as significant shifts in the location of wind farms are not expected.
 193 In total, twelve CF time series were analysed in this study, six for individual
 194 wind and PV CF (three datasets for each source) in the 91W-9PV scenario,
 195 and an additional six time series that include the combined CF for 91W-9PV
 196 and 57W-43PV scenarios across the different datasets.

197 It is important to note that the specific capacity values used in this study
 198 are illustrative and are not intended to reflect precise future realities. Instead,
 199 they serve to explore the impact of transitioning from a wind-dominated sys-
 200 tem (91W-9PV) to a more evenly distributed system (57W-43PV). This ap-
 201 proach allows for a comparative analysis between the two scenarios, assessing
 202 how the balance of RES capacity affects the occurrence of RES droughts.

203 3.5. *RES Drought Definition*

204 In this study, a RES drought event was defined as occurring when the
 205 24-hour moving average of CF remains below a fixed threshold of 0.1 for
 206 a period of longer than 24 hours. The choice of this threshold is somewhat
 207 arbitrary, but aligns with similar studies on low renewable energy production
 208 [4, 6, 7]. By using a 24-hour moving average, fewer but longer-lasting events
 209 were captured compared to using the raw CF time series, which can be more
 210 sensitive to short-term fluctuations. A fixed threshold approach was chosen
 211 in this study to enable consistent inter-comparison between datasets.

212 The moving average approach smooths out short-term fluctuations, so
 213 that brief periods above the threshold do not interrupt an otherwise con-
 214 tinuous low-CF period (Fig. 1). This means that a single hour above the
 215 threshold does not "break" a drought event if it is surrounded by prolonged
 216 low-generation hours. As a result, fewer but longer-lasting drought events

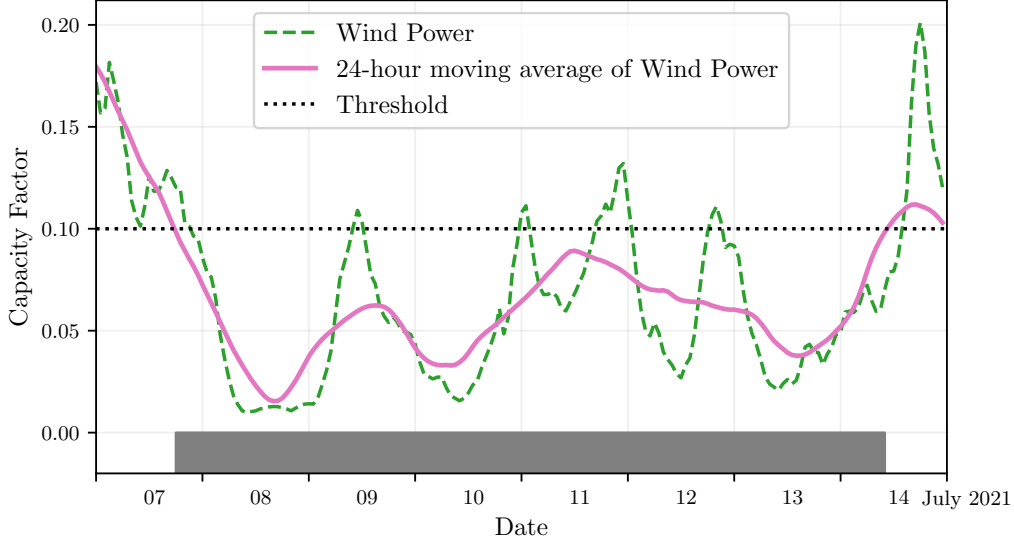


Figure 1: Wind time series of CF (green) and its 24-hour moving average (pink) from the 7th to the 15th of July 2021. The black dashed line indicates the CF threshold. The grey bar shows the period identified as a wind drought under our definition

are identified, which may better reflect real-world conditions where energy supply constraints persist over extended periods.

4. Results

4.1. Verification

The accuracy of the datasets used in this study was verified, before continuing to the analysis of RES droughts. For the verification process, time-varying values of installed capacity were used to account for changes in RES development over the verification period. This step allowed us to assess how well the datasets represent the production of renewable energy by comparing them against observed data.

4.1.1. Wind Energy

The C3S-E datasets use the Vestas V136/3450 wind turbine power curve, (Fig. 2a). The Atlite model allows the user to specify the power curve. We considered the 121 power curves available for download from Renewables.ninja [26]. For each power curve, Renewables.ninja also provides four

232 associated smoothed power curves. The smoothing is done using a Gaussian
 233 filter with different standard deviations that depend on the wind speed. A
 234 separate wind CF time series for Ireland was generated for each of the wind
 235 turbine power curves and smoothing levels.

236 The performance of each CF time series is then assessed based on four skill
 237 scores: correlation coefficient (CC), root mean square error (RMSE), mean
 238 bias error (MBE), and the percentage of overlap. The percentage of overlap
 239 quantifies the similarity between the observed and modelled distributions. It
 240 is a positively oriented skill score, where 100% shows full agreement between
 241 the two distributions, and 0% indicates no overlap. The histograms of hourly
 242 CF values for the most recent decade (2014-2023) are used to calculate this
 243 skill score.

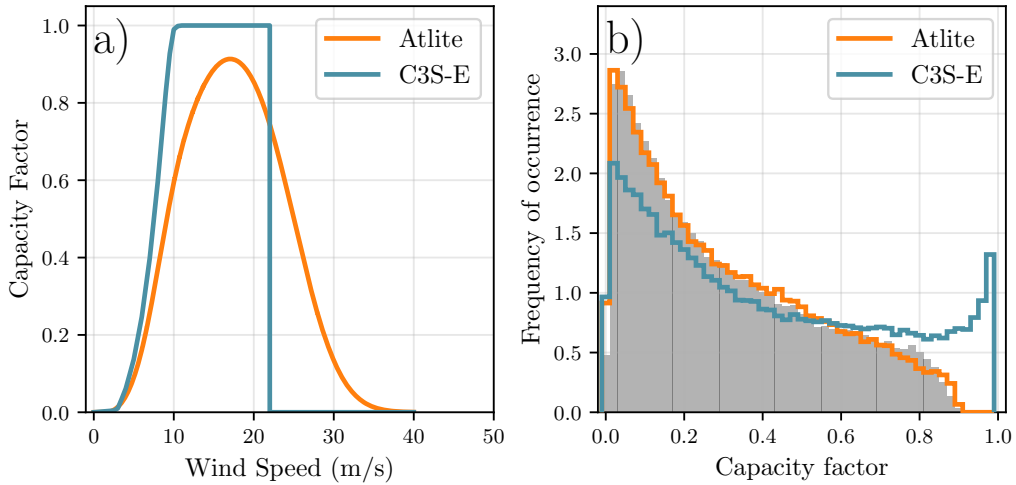


Figure 2: a) Power curves of the Enercon E112.4500 with a $0.3w$ smoothing filter used by Atlite (orange) and the Vestas V136/3450 used by C3S-E (blue) b) Histograms of wind CF for Ireland from Atlite (orange), C3S-E (blue) and Observed (shaded)

244 Based on these metrics, the most representative power curve for Ireland
 245 is the Enercon E112.4500 power curve with the $0.3w$ smoothing filter. The
 246 smoothing of the wind turbine power curve represents losses associated with
 247 each turbine, as well as losses such as wake effects between turbines, which
 248 are important when modelling wind energy on larger spatial scales. The his-
 249 togram in Fig. 2b shows that the C3S-E power curve tends to underestimate
 250 low CF values and overestimate higher ones, whereas the smoothed Atlite

251 power curve more closely follows the observed wind availability data. This
 252 is further supported by the percentage of overlap which is higher for Atlite
 253 (97.2%) than for C3S-E (83.2%), indicating better agreement with observed
 254 data.

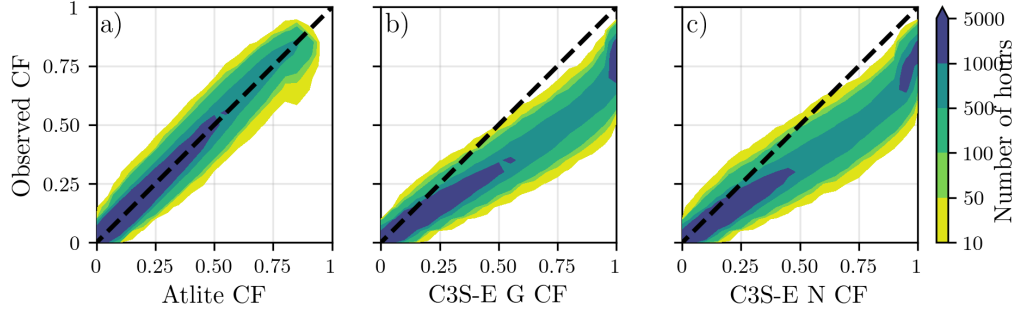


Figure 3: Wind CF density plot of the observed CF (vertical axes) and modelled (horizontal axes) CF data for the a) Atlite, b) C3S-E G and c) C3S-E N datasets

255 The effect of the difference between the power curves is also visible in
 256 Fig. 3, which shows a density plot of wind CF values. The two C3S-E datasets
 257 are shown to overestimate the observed CF, whereas the Atlite model is in
 258 good agreement with the observed data. The skill scores presented in Table 2
 259 show that Atlite performs better than the C3S-E datasets for all of the skill
 260 scores.

	Atlite	C3S-E G	C3S-E N
CC	0.981	0.972	0.970
RMSE	0.045	0.177	0.162
MBE	-0.003	0.137	0.121

Table 2: Skill scores for wind power for the three datasets compared to observed data

261 Fig. 4 shows the average annual number of wind drought events during
 262 the 2014 to 2023 validation period. The figure reveals that Atlite presents
 263 the best overall agreement with the observed frequency and duration of wind
 264 drought events. This pattern is particularly evident for shorter-duration
 265 events, which are the most frequent.

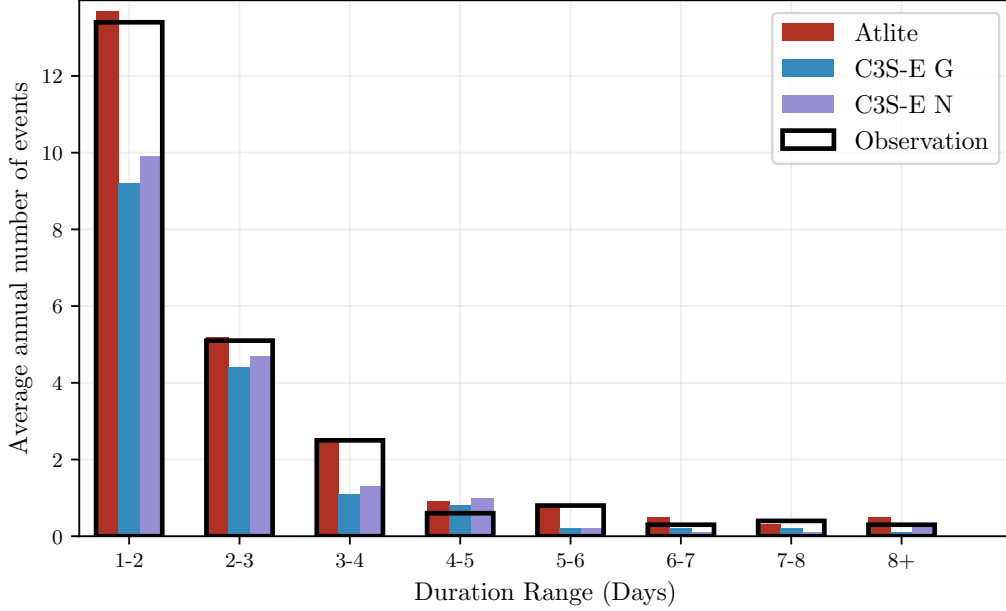


Figure 4: Average annual number of wind drought events for Atlite (red), C3S-E G (blue), C3S-E N (purple), and the observed data (black outline). The wind droughts are identified from 2014 to 2023, considering the actual capacity of the system at any given time

4.1.2. PV Energy

The Atlite model allows the user to select certain PV panel characteristics. In this study, the three PV panel types available in the Atlite model were considered (CSi, CdTe, Kaneka). Following the same methodology as in the previous section, the three available models were compared using four skill scores (CC, RMSE, MBE, and the percentage of overlap). Based on the best-performing metrics, the Beyer PV panel model was selected [29], using the Kaneka Hybrid panel option. For all PV farm locations, the azimuth angle is fixed at 180° (due south), and the optimal tilt angle option is applied.

The PV installed capacity available on the spreadsheets from EirGrid represents the Maximum Export Capacity (MEC) and does not accurately reflect the installed PV capacity. To enable actual PV generation potential to be modelled correctly, installed capacities were set at 1.4 times the MEC values. This scaling factor was estimated by analysing proprietary data from individual PV farms provided by EirGrid, which showed that, on average, assuming that the installed capacities of farms exceed their MEC values by

282 40% yields the best agreement with the observed availability.

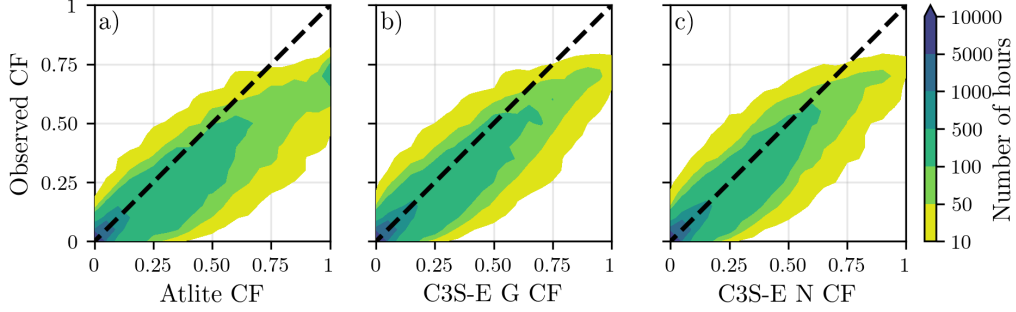


Figure 5: PV CF density plot of the observed (vertical axes) and modelled (horizontal axes) CF series for the a) Atlite, b) C3S-E G and c) C3S-E N datasets

283 Figure 5 shows that the three datasets have a similar tendency to overesti-
 284 mate the CF compared to the observed values, especially for high CF values.
 285 The skill scores presented in Table 3 indicate that C3S-E G performs best
 286 overall, with the lowest RMSE and a high correlation coefficient, suggesting
 287 a closer match to observed data. All models show a slight positive bias, with
 288 Atlite exhibiting a slightly lower correlation and higher RMSE.

	Atlite	C3S-E G	C3S-E N
CC	0.921	0.931	0.931
RMSE	0.119	0.090	0.113
MBE	0.046	0.027	0.021

Table 3: Skill scores for PV CF for the three datasets compared to observed data

289 Fig. 6 shows the number of PV drought events during the 2023 validation
 290 period across different duration ranges. The figure reveals partial agreement
 291 between the three datasets and the observed data, with consistent results
 292 noticed for duration ranges of 1-2, 3-4, 7-8, and 8+ days. However, dis-
 293 crepancies appear in the other ranges, where the models diverge from the
 294 observed data. The main challenge in validating PV data stems from the
 295 recent installation of a large share of Ireland’s PV capacity, with over 65%
 296 of the total PV capacity installed in 2023. This results in uncertainties in PV
 297 generation data and the actual generating capacity in the first few months
 298 after each farm is connected.

299 As the goal of this analysis is to assess the combination of wind and PV
 300 generation, the complementary nature of these energy sources mitigates the
 301 limitations in PV-only results.

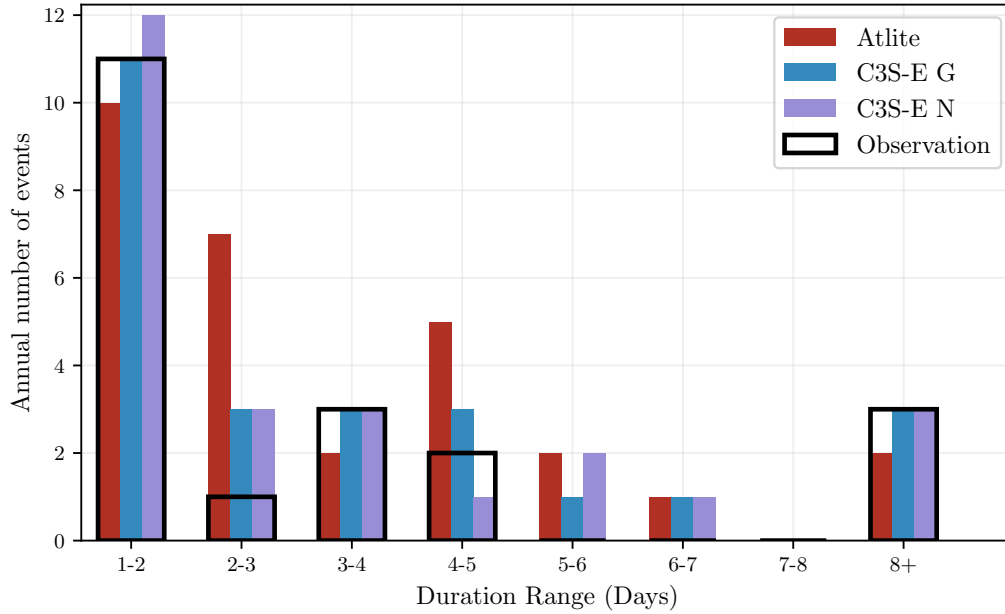


Figure 6: Number of PV drought events for Atlite (red), C3S-E G (blue), and C3S-E N (purple) and the observed data (black outline). The PV droughts are identified for 2023, considering the actual capacity of the system at any given time

302 4.2. Analysis

303 In this section, RES drought events are evaluated under two different
 304 scenarios with fixed installed capacities: the 91W-9PV scenario, with 5.9 GW
 305 of wind capacity and 0.6 GW of PV capacity; and the 57W-43PV scenario,
 306 where wind capacity comprises 11.45 GW and PV capacity increases to 8.6
 307 GW. Both scenarios were driven by 45 years of ERA5 data. Using the RES
 308 drought identification process described in Section 3.5, wind and PV droughts
 309 are first analysed separately before presenting the results for combined (wind
 310 + PV) RES droughts under both scenarios.

311 4.2.1. Annual Number of RES Droughts

312 The analysis of annual RES drought events reveals trends that are largely
 313 consistent with earlier studies. When only wind energy is considered (Fig.7a),

the number of drought events decreases as the duration range increases, with very few events lasting more than seven days. This pattern aligns with previous research showing that wind droughts tend to be short and frequent. In contrast, for PV energy (Fig.7b), drought frequency declines from one to eight days and then slightly increases for longer durations. This behaviour is attributable to Ireland’s high-latitude location, where reduced sunlight in winter (from November to March) leads to consistently low PV output.

Moreover, the comparison between wind and PV results indicates that the median, first, and third quartiles for PV are consistently higher than or equal to those for wind. This is expected, given that PV generation is inherently lower, zero at night, and limited by the solar cycle, as observed in other studies. When wind and PV are combined under the 91W-9PV scenario (Fig.7c), the results closely mirror those of wind alone, reaffirming wind’s dominance in the current energy mix. However, in the 57W-43PV scenario (Fig.7d), a marked reduction in drought events is observed across all datasets, with a decrease of the total number of events of 56% for Atlite, 52% for C3S-E G, and 50% for C3S-E N, demonstrating the beneficial effects of a more balanced energy mix. These findings are in line with earlier studies that highlight how increasing PV capacity can mitigate drought frequency through the anti-correlated seasonal patterns of wind and solar generation.

Additionally, the consistently higher drought counts reported by the Atlite dataset, compared to the C3S-E datasets, underscore the impact of model selection, particularly the influence of wind turbine power curve representation, on quantifying RES droughts. This observation is consistent with previous research, which has also noted that assumptions regarding turbine characteristics can significantly affect drought duration estimates.

4.2.2. Return Periods of RES Drought Duration

The RES drought events identified over the 45-year period were used to calculate the return periods for different RES drought durations. A return period is the estimated average time interval between events of a specified duration or intensity (not to be confused with the frequency of their occurrence within a fixed time frame). Fig. 8 illustrates the return periods for varying RES drought durations, highlighting how often different drought lengths are likely to occur across the datasets. This analysis provides insight into the frequency and likelihood of prolonged low-generation periods, which is crucial for evaluating the impact of extreme RES droughts on system resilience. Understanding these return periods is essential, as even infrequent

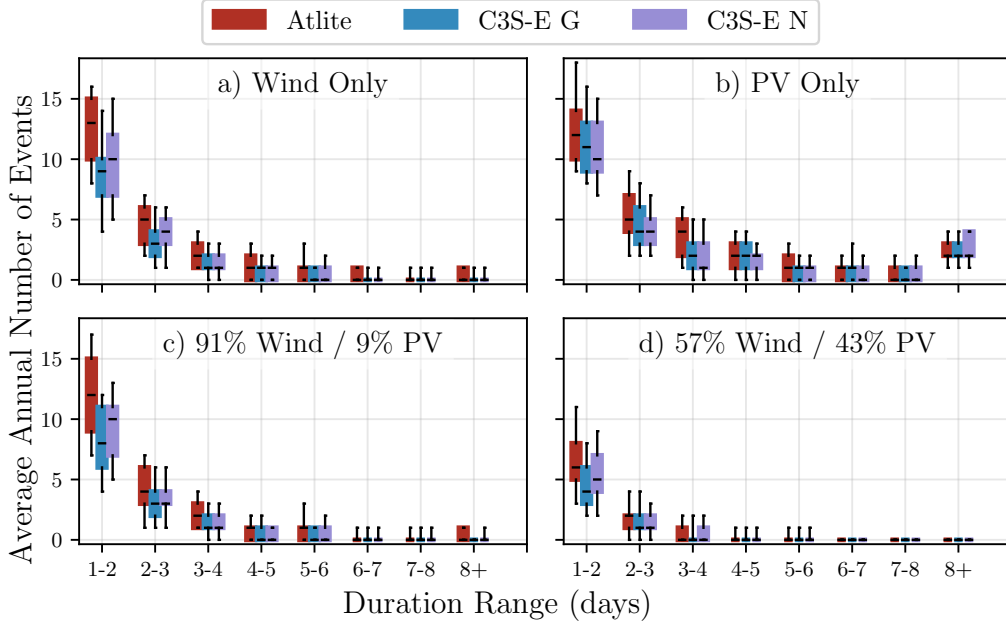


Figure 7: Average annual number of RES droughts (from 1979 to 2023) for a) Wind, b) PV, c) 91W-9PV and d) 57W-43PV for Atlite (red), C3S-E G (blue), and C3S-E N (purple). The x-axis represents duration ranges in days (lower bound included), while the y-axis indicates the annual number of events. The boxes display the first and third quartiles and the median is marked by a black line. The whiskers indicate the 5th and 95th percentiles

can challenge energy security by placing significant strain on conventional backup sources necessary to maintain supply in high-RES scenarios.

For wind (Fig. 8a), the log-linear increase in return periods observed in this study confirms that longer droughts occur exponentially less frequently, a trend consistent with earlier research on wind variability. In the case of PV droughts (Fig. 8b), the Atlite dataset shows a generally log-linear trend, while the C3S-E datasets exhibit a sudden increase in drought duration for events exceeding sixteen days. This abrupt rise reflects differences in how PV output is handled near the CF threshold during low irradiance conditions. Interestingly, when the share of wind power is decreased in the balanced scenario, the overall return periods for drought events increase. Although wind energy is generally more stable, reducing its share makes the combined system more vulnerable to PV's extended low-generation periods in winter. This highlights that the seasonal limitations of PV can dominate the overall

365 drought characteristics when its share increases, emphasizing the importance
 366 of carefully balancing the energy mix for RES drought risk assessment.

367 Under the 91W-9PV scenario (Fig. 8c), the combined RES drought return
 368 periods largely mirror those for wind alone, reflecting the dominance of wind
 369 in the current energy mix. In contrast, the balanced 57W-43PV scenario
 370 (Fig. 8d) shows a dramatic increase in return periods across all durations,
 371 suggesting that a more diversified energy mix can substantially mitigate the
 372 frequency of prolonged drought events.

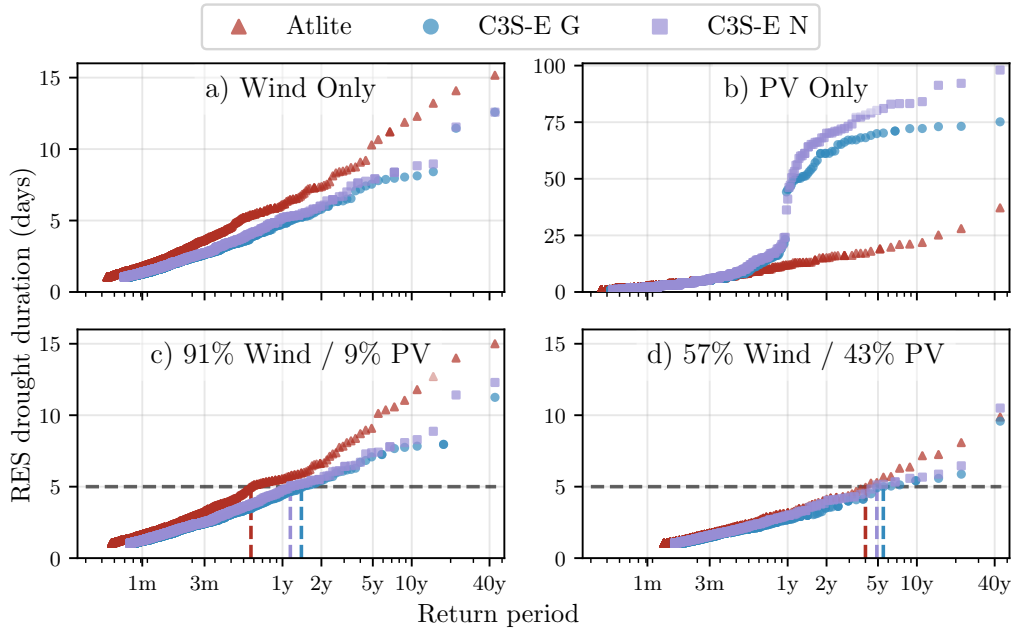


Figure 8: Return periods of the duration of RES droughts (from 1979 to 2023) for a) Wind, b) PV, c) 91W-9PV and d) 57W-43PV for Atlite (red triangle), C3S-E G (blue circle), and C3S-E N (purple square). The x-axis represents the return period time in a log-scale and the y-axis indicates the duration of RES drought associated with it. The horizontal dashed line marks the 5-day return period, with coloured vertical dashed marking its return period for each dataset

373 Across Fig. 8a, c, and, d, the return periods in the Atlite dataset are
 374 consistently higher than those in the two C3S-E datasets. For instance, in
 375 the 91W-9PV scenario (Fig. 8c), an event with a one-year return period
 376 lasts six days in the Atlite dataset, compared to only five days in the C3S-E
 377 datasets. This difference underscores the importance of model selection when

quantifying RES droughts, as each model’s assumptions and parametrisations significantly influence drought duration estimates. Additionally, in all four graphs, the similarity between results from the two C3S-E datasets suggests that assumptions in the Atlite model, such as wind turbine power curve selection and PV panel specifications, have a greater impact on RES drought duration estimates than the precise geographic distribution of RES farms when studying the return periods of RES droughts.

4.2.3. Seasonal Distribution of RES Droughts

The seasonal analysis of RES droughts is based on the percentage of hours in each month classified as drought events. For the wind-only scenario (Fig. 9a), the Atlite dataset exhibits a pronounced seasonal pattern, with about 24% of summer hours (June–July–August) identified as droughts compared to only 4% in winter (December–January–February). This strong seasonal signal is less evident in the C3S-E datasets, which suggests that the differences in the underlying wind power curves play a significant role. In Atlite, CF near or below the 0.1 threshold occur at relatively higher wind speeds, resulting in a higher count of drought hours during the summer months.

In contrast, PV droughts (Fig. 9b) display an opposite seasonal trend. Across all datasets, over 60% of winter hours are classified as PV droughts, reflecting the naturally low solar irradiance in Ireland during winter. Moreover, Atlite tends to record a slightly higher percentage of drought hours for wind and a marginally lower percentage for PV relative to the C3S-E datasets. These differences highlight how model-specific assumptions, such as the treatment of wind turbine power curves and PV panel characteristics, significantly influences the apparent seasonal dynamics of RES droughts.

The 91W-9PV scenario (Fig. 9c) shows patterns comparable to the ones for wind droughts (Fig. 9a). However, in the 91W/9PV scenario, the number of hours classified as RES droughts in summer decreases slightly compared to the wind-only scenario. This reduction can be explained by the contribution of PV generation during the summer months in the 91W-9PV scenario, even though it constitutes only 11% of total capacity. Since the number of RES drought hours for PV in summer is near zero, this small contribution has a noticeable impact on reducing overall drought hours. In the 57W-43PV scenario (Fig. 9d), all three datasets show a reduction in monthly RES drought frequency. Annual reductions in median RES drought frequency are observed across the datasets, dropping from 14% to 5% for Atlite, from 8% to 3% for

415 C3S-E G, and from 9% to 4% for C3S-E N. The balanced mix of wind and
 416 PV power in this scenario reduces the seasonal signal overall and significantly
 417 decreases the percentage of RES drought hours in the summer.

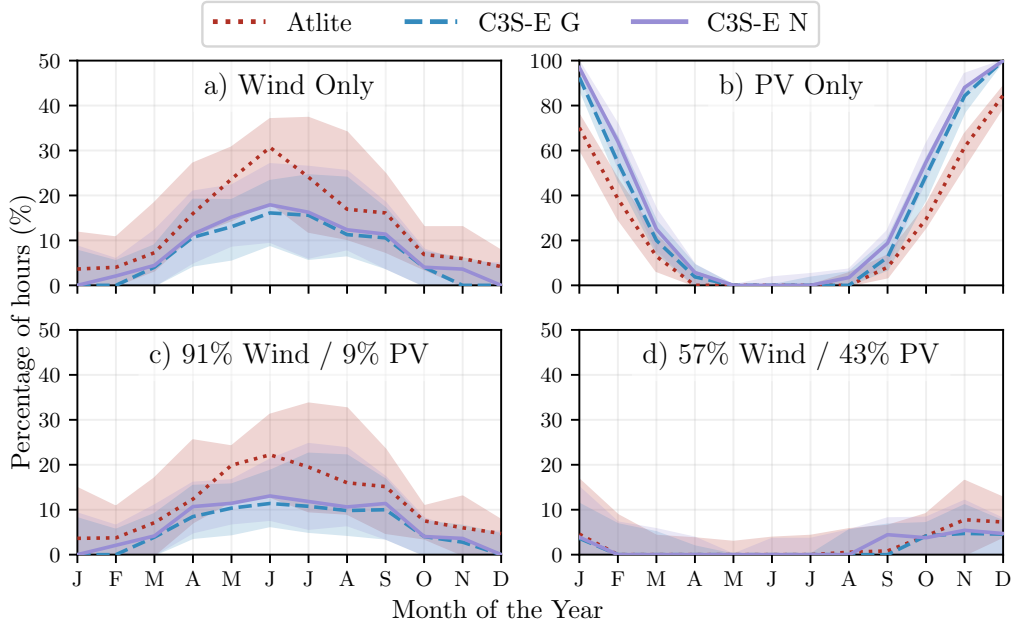


Figure 9: Percentage of hours in a month which are part of a RES drought (from 1979 to 2023) for a) Wind, b) PV, c) 91W-9PV and d) 57W-43PV for Atlite (red dotted), C3S-E G (blue dashed), and C3S-E N (purple solid). The x-axis represents the month of the year, and the y-axis indicates the percentage of hours. Lines correspond to the median values and the area between the first and third quartiles is shaded. Note the different y-axis scale for b).

418 The seasonal variations observed in this study have important implica-
 419 tions for energy planning. Given that energy demand peaks in winter for
 420 Northern European countries, understanding these seasonal patterns is criti-
 421 cal for assessing the need for conventional backup or storage solutions during
 422 periods of prolonged low renewable output. The findings underscore that
 423 even small differences in model assumptions leads to significant variations in
 424 drought estimates, thereby affecting the reliability of the energy system dur-
 425 ing critical periods. Such insights are essential for policymakers to develop
 426 targeted strategies that enhance grid resilience and ensure a stable energy
 427 supply throughout the year.

428 5. Conclusions

429 This study has investigated the ability of three RES datasets to repre-
430 sent RES droughts: Atlite, C3S-E G, and C3S-E N. One of the most evident
431 differences is how each dataset incorporates the specific locations of RES
432 farms. Both Atlite and C3S-E G consider the locations of wind and PV
433 farms, which one would expect to result in a more accurate representation
434 of RES generation. While this approach slightly improves PV models, our
435 analysis indicates that for wind energy, the Atlite dataset performs better
436 overall, especially in its close alignment with observed data for wind gener-
437 ation estimates. This finding suggests that, although the inclusion of RES
438 farm locations is beneficial, the accuracy of the RES dataset is more strongly
439 influenced by underlying model assumptions, such as selecting an appropriate
440 wind power curve.

441 Atlite shows the best alignment with observed data for wind generation.
442 Differences between the datasets are smaller for PV, with C3S-G perform-
443 ing marginally better than the other two. The results show that the two
444 C3S-E datasets (C3S-E G and C3S-E N) consistently yield similar outcomes,
445 indicating that their methodological differences have minimal impact in this
446 case. This distinction is also evident in the analysis, where Atlite reports
447 higher return periods and a greater number of RES droughts, especially in
448 scenarios with a balanced share of RES. Again, the results from RES drought
449 modelling rely more on the precision of the wind power curve and PV panel
450 models than on the specific locations of RES farms. Atlite’s superior perfor-
451 mance highlights the importance of selecting validated models for assessing
452 RES drought risks. This careful model selection can better quantify risks,
453 support effective planning, and avoid the potential underestimation of ca-
454 pacity needs, which is essential for ensuring energy security.

455 Looking at the 57W-43PV scenario, the analysis showed a significant im-
456 provement in the management of RES droughts due to the complementary
457 nature of wind and PV generation. Wind and PV together perform better
458 in terms of reducing drought frequency and duration than either would in-
459 dividualy, largely because of the seasonal anti-correlation between the two
460 energy sources. This diversification reduces the seasonal impact on RES
461 droughts, as PV generation peaks in the summer and wind generation is
462 more consistent in winter. Ireland currently has a highly wind-dependent
463 energy system, but with ambitious targets for PV installations in the coming
464 years, the energy mix is expected to approach a balance between wind and

PV capacity. While this balanced approach offers a more stable and secure energy supply by mitigating RES drought risks, it is important to note that having similar wind and PV capacities may not optimise other aspects, such as annual energy production or meeting nighttime loads. For policymakers, these findings underscore the importance of meeting these capacity targets to enhance energy security through diversification. Additionally, the choice of model for RES drought assessment becomes increasingly critical as more renewable capacity is integrated into the system.

This study has several limitations. Although ERA5 is among the best reanalysis datasets for renewable energy analysis [?], its resolution may not capture local-scale phenomena, making it less reliable at the individual farm level. In addition, our methodology employs a fixed threshold to define RES drought events, which is necessary to compare the three models but does not account for demand variations. Consequently, while this approach enables a consistent inter-comparison, it may overlook events that are most critical for power system operations.

Future work is planned to extend the current analysis. First, climate projection data will be integrated with different energy scenarios, incorporating the addition of offshore wind, to better understand how climate change might affect RES droughts. Second, expanding the geographic domain of the study to include the rest of Europe would provide a more comprehensive understanding of RES droughts in an interconnected energy grid. This would require extensive verification across other European countries, making it a more complex but highly relevant challenge.

Data Availability

The ERA5 data can be obtained from the Climate Data Store (<https://doi.org/10.24381/cds.adbb2d47>). The C3S-E dataset is also available from the Climate Data Store (<https://doi.org/10.24381/cds.4bd77450>). Information on wind and PV farms in Ireland can be obtained from the EirGrid website (<https://www.eirgrid.ie/grid/system-and-renewable-data-reports>). The Atlite model used in this study is open-source and can be found on GitHub (<https://github.com/pypsa/atlite>). The data and code required to reproduce the analysis in this article will be made available upon acceptance of the manuscript in a public GitHub repository.

499 Acknowledgments

500 The research conducted in this publication was funded by Science Foun-
501 dation Ireland and co-funding partners under grant number 21/SPP/3756
502 through the NexSys Strategic Partnership Programme.

503 References

- 504 [1] EuroStat, Renewable Energy Statistics, 2023. URL: https://ec.europa.eu/eurostat/statistics-explained/index.php?title=Renewable_energy_statistics, Accessed: 2024-11-06.
- 505
506
- 507 [2] H. C. Bloomfield, D. J. Brayshaw, L. C. Shaffrey, P. J. Coker, H. E. Thornton, Quantifying the increasing sensitivity of power systems to climate variability, *Environmental Research Letters* 11 (2016) 124025. doi:10.1088/1748-9326/11/12/124025.
- 508
509
510
- 511 [3] H. C. Bloomfield, D. J. Brayshaw, A. Troccoli, C. M. Goodess, M. De Felice, L. Dubus, P. E. Bett, Y.-M. Saint-Drenan, Quantifying the sensitivity of european power systems to energy scenarios and climate change projections, *Renewable Energy* 164 (2021) 1062–1075. doi:10.1016/j.renene.2020.09.125.
- 512
513
514
515
- 516 [4] F. Kaspar, M. Borsche, U. Pfeifroth, J. Trentmann, J. Drücke, P. Becker, A climatological assessment of balancing effects and shortfall risks of photovoltaics and wind energy in germany and europe, *Advances in Science and Research* 16 (2019) 119–128. doi:10.5194/asr-16-119-2019.
- 517
518
519
520
- 521 [5] F. Mockert, C. M. Grams, T. Brown, F. Neumann, Meteorological conditions during periods of low wind speed and insolation in Germany: The role of weather regimes, *Meteorological Applications* 30 (2023) e2141. doi:10.1002/met.2141.
- 522
523
524
- 525 [6] M. Ohba, Y. Kanno, D. Nohara, Climatology of dark doldrums in japan, *Renewable and Sustainable Energy Reviews* 155 (2022) 111927. doi:10.1016/j.rser.2021.111927.
- 526
527
- 528 [7] M. J. Mayer, B. Biró, B. Szücs, A. Aszódi, Probabilistic modeling of future electricity systems with high renewable energy penetration using
- 529

- 530 machine learning, *Applied Energy* 336 (2023) 120801. doi:10.1016/j.
531 apenergy.2023.120801.
- 532 [8] D. Raynaud, B. Hingray, B. François, J. Creutin, Energy droughts from
533 variable renewable energy sources in European climates, *Renewable*
534 *Energy* 125 (2018) 578–589. doi:[https://doi.org/10.1016/j.renene](https://doi.org/10.1016/j.renene.2018.02.130)
535 .2018.02.130.
- 536 [9] A. Gangopadhyay, A. K. Seshadri, N. J. Sparks, R. Toumi, The role
537 of wind-solar hybrid plants in mitigating renewable energy-droughts,
538 *Renewable Energy* 194 (2022) 926–937. doi:10.1016/j.renene.2022.
539 05.122.
- 540 [10] J. Kapica, J. Jurasz, F. A. Canales, H. Bloomfield, M. Guezgouz,
541 M. De Felice, Z. Kobus, The potential impact of climate change on
542 european renewable energy droughts, *Renewable and Sustainable En-*
543 *ergy Reviews* 189 (2024) 114011. doi:10.1016/j.rser.2023.114011.
- 544 [11] K. Z. Rinaldi, J. A. Dowling, T. H. Ruggles, K. Caldeira, N. S. Lewis,
545 Wind and Solar Resource Droughts in California Highlight the Benefits
546 of Long-Term Storage and Integration with the Western Interconnect,
547 *Environmental Science and Technology* 55 (2021) 6214–6226. doi:10.1
548 021/acs.est.0c07848.
- 549 [12] P. T. Brown, D. J. Farnham, K. Caldeira, Meteorology and climatology
550 of historical weekly wind and solar power resource droughts over western
551 North America in ERA5, *SN Applied Sciences* 3 (2021) 814. doi:10.1
552 007/s42452-021-04794-z.
- 553 [13] S. Allen, N. Otero, Standardised indices to monitor energy droughts,
554 *Renewable Energy* 217 (2023) 119206. doi:10.1016/j.renene.2023.11
555 9206.
- 556 [14] C. Bracken, N. Voisin, C. D. Burleyson, A. M. Campbell, Z. J. Hou,
557 D. Broman, Standardized benchmark of historical compound wind and
558 solar energy droughts across the Continental United States, *Renewable*
559 *Energy* 220 (2024) 119550. doi:[https://doi.org/10.1016/j.renene](https://doi.org/10.1016/j.renene.2023.119550)
560 .2023.119550.
- 561 [15] H. Lei, P. Liu, Q. Cheng, H. Xu, W. Liu, Y. Zheng, X. Chen, Y. Zhou,
562 Frequency, duration, severity of energy drought and its propagation in

- 563 hydro-wind-photovoltaic complementary systems, *Renewable Energy*
564 (2024) 120845. doi:10.1016/j.renene.2024.120845, 2.
- 565 [16] H. Hersbach, B. Bell, P. Berrisford, S. Hirahara, A. Horányi, J. Muñoz-
566 Sabater, J. Nicolas, C. Peubey, R. Radu, D. Schepers, et al., The ERA5
567 global reanalysis, *Quarterly Journal of the Royal Meteorological Society*
568 146 (2020) 1999–2049. doi:10.1002/qj.3803.
- 569 [17] L. Dubus, Y. Saint-Drenan, A. Troccoli, M. De Felice, Y. Moreau, L. Ho-
570 Tran, C. Goodess, R. Amaro E Silva, L. Sanger, C3S Energy: A climate
571 service for the provision of power supply and demand indicators for Eu-
572 rope based on the ERA5 reanalysis and ENTSO-E data, *Meteorological*
573 *Applications* 30 (2023) e2145. doi:10.1002/met.2145.
- 574 [18] Copernicus Climate Change Service (C3S), Climate and energy indi-
575 cators for Europe from 1979 to present derived from reanalysis., 2020.
576 doi:10.24381/cds.4bd77450, accessed on 28-11-2024.
- 577 [19] F. Hofmann, J. Hampp, F. Neumann, T. Brown, J. Hörsch, Atlite: a
578 lightweight Python package for calculating renewable power potentials
579 and time series, *Journal of Open Source Software* 6 (2021) 3294. doi:10
580 .21105/joss.03294.
- 581 [20] J. Li, Z. Zhao, D. Xu, P. Li, Y. Liu, M. A. Mahmud, D. Chen, The
582 potential assessment of pump hydro energy storage to reduce renewable
583 curtailment and CO2 emissions in Northwest China, *Renewable Energy*
584 212 (2023) 82–96. doi:10.1016/j.renene.2023.04.132.
- 585 [21] M. Parzen, H. Abdel-Khalek, E. Fedotova, M. Mahmood, M. M. Frysz-
586 tacki, J. Hampp, L. Franken, L. Schumm, F. Neumann, D. Poli,
587 et al., Pypsa-earth. a new global open energy system optimization
588 model demonstrated in africa, *Applied Energy* 341 (2023) 121096.
589 doi:10.1016/j.apenergy.2023.121096.
- 590 [22] K. Ali Khan Niazi, M. Victoria, Comparative analysis of photovoltaic
591 configurations for agrivoltaic systems in europe, *Progress in Photo-*
592 *voltatics: Research and Applications* 31 (2023) 1101–1113. doi:10.1002/
593 pip.3727.

- 594 [23] EirGrid & SONI, System and Renewable Data Reports, 2023. URL:
595 [https://www.eirgrid.ie/grid/system-and-renewable-data-rep](https://www.eirgrid.ie/grid/system-and-renewable-data-reports)
596 [orts](https://www.eirgrid.ie/grid/system-and-renewable-data-reports), Accessed: 2024-11-06.
- 597 [24] N. Otero, O. Martius, S. Allen, H. Bloomfield, B. Schaeffli, Character-
598 izing renewable energy compound events across Europe using a logistic
599 regression-based approach, *Meteorological Applications* 29 (2022) e2089.
600 doi:10.1002/met.2089, 13.
- 601 [25] Y.-M. Saint-Drenan, L. Wald, T. Ranchin, L. Dubus, A. Troccoli, An
602 approach for the estimation of the aggregated photovoltaic power gener-
603 ated in several European countries from meteorological data, *Advances*
604 *in Science and Research* 15 (2018) 51–62. doi:10.5194/asr-15-51-201
605 8.
- 606 [26] I. Staffell, S. Pfenninger, Using bias-corrected reanalysis to simulate
607 current and future wind power output, *Energy* 114 (2016) 1224–1239.
608 doi:10.1016/j.energy.2016.08.068.
- 609 [27] Government of Ireland, Climate Action Plan 2024, Technical Report 3,
610 Department of the Environment, Climate and Communications, 2023.
611 URL: [https://www.gov.ie/pdf/?file=https://assets.gov.ie/](https://www.gov.ie/pdf/?file=https://assets.gov.ie/284675/70922dc5-1480-4c2e-830e-295afd0b5356.pdf)
612 [284675/70922dc5-1480-4c2e-830e-295afd0b5356.pdf](https://www.gov.ie/pdf/?file=https://assets.gov.ie/284675/70922dc5-1480-4c2e-830e-295afd0b5356.pdf), Accessed:
613 2024-11-06.
- 614 [28] Sustainable Energy Authority Ireland, National Energy Projections
615 2024, Technical Report, Sustainability Energy Authority of Ireland,
616 2024. URL: [https://www.seai.ie/news-and-events/news/energ](https://www.seai.ie/news-and-events/news/energy-projections-report)
617 [y-projections-report](https://www.seai.ie/news-and-events/news/energy-projections-report), Accessed: 2024-11-06.
- 618 [29] H. G. Beyer, G. Heilscher, S. Bofinger, A robust model for the mpp
619 performance of different types of pv-modules applied for the performance
620 check of grid connected systems, *Eurosun* (2004) 8.